ACS APPLIED MATERIALS & INTERFACES

Research Article

www.acsami.org

Ice-phobic Coatings Based on Silicon-Oil-Infused Polydimethylsiloxane

Lin Zhu,[†] Jian Xue,[†] Yuanyi Wang,[†] Qingmin Chen,[†] Jianfu Ding,[‡] and Qingjun Wang*[,†]

[†]Department of Polymer Science & Engineering, School of Chemistry and Chemical Engineering, Nanjing University, Nanjing 210093

[‡]Security and Disruptive Technologies, National Research Council Canada, 1200 Montreal Road, Ottawa, Ontario K1A 0R6, Canada

Supporting Information

ABSTRACT: A simple and low-cost technique for the preparation of silicon-oil-infused polydimethylsiloxane (PDMS) coatings with different silicon oil contents have been developed and studied. This material is designed for ice-phobic applications, and thus a high hydrophobic property of PDMS is maintained by avoiding any polar groups such as C═O and OH in the structure. Therefore, the polymer main chain was attached with vinyl and Si−H groups to obtain a cross-linking capability, meanwhile to ensure a nonpolar chemical structure. Its ice-phobic property has been investigated in terms of ice adhesion strength (tensile and shear), water contact angle, icing dynamics using high-speed photography and morphology using TEM, SEM and AFM. The prepared coating surface shows a low surface energy and very low ice adhesion strength of 50 kPa, only about 3% of the value on a bare aluminum (Al) surface. In the silicon oil infused PDMS coatings, the low surface energy of the silicon oil and PDMS, and the high mobility of silicon oil played an important role on the ice-phobic property. Both of these factors offer the surface a large water contact angle and hence a small contact area, leading to the formation of a loose ice layer. In addition, the oil infused polymer structure significantly reduces the contact area of the ice with solid substrate since the ice mostly contacts with the mobile oil. This leads to a very weak interaction between the substrate and ice, consequently significantly reduces the ice adhesion strength on the surface. Therefore, such material could be a good candidate for ice-phobic coatings on which the accumulated ice may be easily removed by a nature force, such as wind, gravity, and vibration.

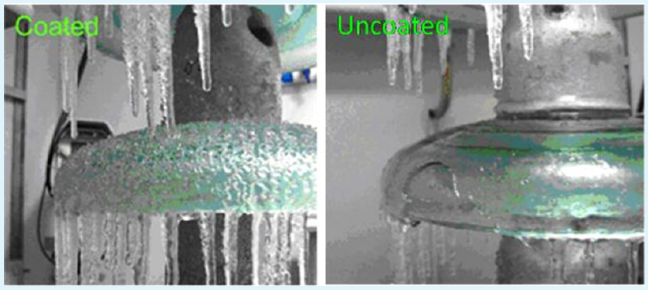

KEYWORDS: *polydimethylsiloxane, silicon oil, oil-infused polymer, hydrophobic, ice-phobic, ice adhesion*

INTRODUCTION

The icing in winter storms in the cold regions of the world frequently causes massive destruction, such as to the electric grid. Many research efforts have been made to solve this problem by either reducing the icing tendency or weakening ice adhesion. It is relatively easy to prevent ice formation on cold objects for a short period of time, but not a long period. Ice will finally accumulate on almost any type of surface under highly condensing weather conditions with low temperatures and high humidity.[1,2] Therefore, investigation techniques to remove the accumulated ice from solid substrates have attracted a lot of attention, and achievements have been reported.[3−5] However, most of the developed methods are based on high energy consumption and some are unfriendly to environment. A better solution to this problem is to reduce the adhesive strength of the formed ice. When the adhesion tensile strength between ice and substrate is decreased to a value lower than 15 psi (100 kPa),[3] the formed ice may be disrupted by a natural force, such as wind, gravity, or vibration, and this type of surface could be used to prevent ice accumulation in winter storms.

It is well-known that a superhydrophobic surface could be a promising ice-phobic system, showing the ability to delay icing for about 2 h. However, it cannot completely prevent ice from forming on the surface, especially under wet and cold weather conditions.[1] Jung et al. reported that a superhydrophobic surface would partially or even completely lose its ice-phobic property under a heavily condensing weather condition.[6] Chen et al. also observed that ice adhesion strength increased with the increase in surface roughness.[7] Moreover, ut was reported that a hydrophobic surface would promote ice nucleation with a rate about 10 times higher than a hydrophilic surface.[8] Our previous work also indicated that ice could build up on many solid surfaces, including superhydrophobic surfaces,[9−11] especially in a low temperature and high humidity environments.[12] Recently, Michael et.al suggested that the reduced ice-phobic property of a superhydrophobic surface was related to the loss of the air voids in the porous structure of the surface between ice and substrate.[13] This is actually caused by the water condensation in the porous nanostructure of the superhydrophobic surface. The condensed water in the pores roots the water on the surface into the porous

Received: October 2, 2012
Accepted: April 22, 2013
Published: April 22, 2013

   dx.doi.org/10.1021/am400704z | ACS Appl. Mater. Interfaces 2013, 5, 4053−4062

Scheme 1. Chemical Structures of PDMS-V and PDMS-H

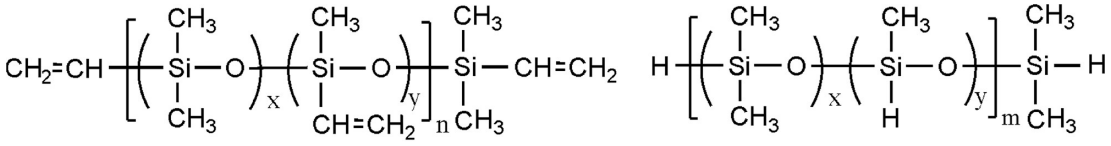

PDMS-V x/y = 0.985/0.015 PDMS-H x/y = 0.9/0.1

structure and finally anchors the ice with the surface after freezing, leading to an increased ice adhesion strength. Obviously this problem would be solved if the water condensation in the porous structure can be prevented. Therefore, a smooth hydrophobic surface may have a better performance as an ice-phobic material, though it would lose the superhydrophobic property because of the lack of a rough surface structure. A recent reported technique of liquid-infused porous surfaces (LIPS) emerged as an excellent method for maintaining both superhydrophobic and ice-phobic properties.[14,15] In this material, the nanopores on a superhydrophobic surface were infused with a water-immiscible liquid, and thus when a water droplet was placed on the surface, the air−liquid contact on a superhydrophobic surface was replaced by liquid−liquid contact. It completely eliminated water condensation in the porous structure. Furthermore, because of the immiscible property of the infused liquid with water, the interaction of water with the surface would be kept at a very small level to offer the surface a low CA as well as an excellent ice-phobic performance.[14,15] In this technique, besides the porous surface structure, which plays a critical role in holding the infused liquid, the chemical property of the surface and the infused liquid will also significantly influence the wetting and icing property of the surface. Materials with polar groups such as C═O or OH will build up a intensive interaction with water and have a strong adhesion with ice through hydrogen bonding and van der Waals's forces. Therefore, low-surface-energy materials with nonpolar structure will be beneficial for reducing the ice adhesion strength on LIPS.

In this work, we introduced a LIPS analogous material based on silicon-oil-infused polydimethylsiloxane (PDMS) for ice-phobic coatings. PDMS itself possesses a lower surface energy with excellent overall properties such as ease for processing, good weather and chemical resistant, excellent insulating and dielectric properties.[16−18] The extremely low glass transition temperature of PDMS ensured this polymer a very large free-volume at an ambient temperature, which would act as voids to accommodate the infused silicon oil to form a LIPS analogous material. In addition, nanosize silica particles were introduced into the material to offer the surface a nanosized roughness to mimic a superhydrophobic surface. Furthermore, a silica-particle-reinforced coating layer was used to obtain an improved mechanical property, which was further promoted by cross-linking. The latter was achieved by a reaction between the vinyl and Si−H groups in the presence of a platinum catalyst. These groups were attached to the main chain of the polymer. The produced silicon-oil-infused PDMS coating showed the weakest interaction with ice reported so far, to the best of our knowledge, and significantly reduced ice adhesion strength from 1500 kPa to 50 kPa (tensile) and 1210 kPa to 40 kPa (shear), dropped by a factor of ∼97%. At this reduced adhesion strength level, the attached ice may fall down under a nature force or be easily removed by consuming little energy. Moreover, the preparation of this type of coating is very simple and cost-effective, avoiding the use of complicated processes such as that used for the preparation of superhydrophic surfaces.

EXPERIMENTAL SECTION

Materials. Octamethylcyclotetrasiloxane (D_4), 2,4,6,8-tetramethylcyclotetrasiloxane (D_4H), 1,1,3,3-tetramethyldisiloxane (MH), 2,4,6,8-tetravinyl-2,4,6,8-tetramethylcyclotetrasiloxane (D_4V), and 1,1,3,3-tetramethyl-1, 3-divinyldisiloxane (MV) were purchased from Xinan Chemical Company. Polydimethylsiloxane (silicon oil) with a weight average molecular weight (M_w) of 6000 Da was purchased from National Chemical Group. Aluminiumtrichloride, tetramethylammonium hydroxide, and chloroplatinic acid were purchased from National Chemical Group. Aluminum plates were purchased from Anometal Aluminum Co. Ltd. China. All other chemicals were analytical grade and used as received.

Surface Modification of the Silica Particles. A fumed silica (CAB-O-SIL LM-150) with an average primary particle diameter of 10−15 nm was purchased from Cabot Corporation. The particles size after dispersing in the polymer matrix was verified to be 20−30 nm by TEM, as will be discussed in the Results and Discussion. The raw fumed silica was surface modified to screen off the polar −OH group on the surface for obtaining a nonpolar surface and for improving the compatibility with PDMS, Therefore, 10 g of the fumed silica was reacted with 60 g of D_4 at 180 °C (240 °C bath temperature) for 2 h with stirring under the protection of nitrogen. After being cooled to room temperature, the reaction mixture was filtered; the collected solid was thoroughly rinsed with toluene three times and then dried under vacuum to yield surface-modified silica particles (nano-SiO_2).

Synthesis of PDMS Resins. A polydimethylsiloxane containing 1.5 mol % vinyl group (PDMS-V, see Scheme 1) was synthesized by bulk copolymerization based on a reported method.[19−22] Briefly, in a 250 mL three-neck flask equipped with a mechanical stirrer, 100 g of D_4, 2.75 g of D_4V, 0.01 g of MV, and 0.02 g of tetramethylammonium hydroxide were added. The reaction was conducted at 110 °C for 12 h under the protection of nitrogen. At the end of the reaction, small molecules and monomer residuals were removed by vacuum distillation. A similar procedure was also used to prepare a Si−H (10 mol %) containing polydimethylsiloxane (PDMS-H) from D_4, D_4H, and MH.

To obtain an extended storage time, a two-part curable PDMS resin for coating was prepared. Therefore, 70 g of PDMS-V was mixed with 30 g of nano-SiO_2 and homogenized by a speedmixer (Siemens, DAC150FV, Germany) at a speed of 3500 rpm for 5 min to ensure a good dispersion of the nano-SiO_2. Half of the mixture was then blended with 1.0 mg of the platinum−siloxane complex catalyst to form Part A, and the other half was mixed with 10.3 g of PDMS-H to form Part B. The platinum−siloxane complex was synthesized using a method described in the literature.[23] This catalyst showed a high activity for this cross-linking reaction and only 10 ppm concentration is required.

Preparation of Coatings. Parts A and B with equivalent PDMS-V and PDMS-H were mixed by a speedmixer at the speed of 3500 rpm for 5 min. For the preparation of silicon oil infused coating, a designed amount of silicon oil was also added to the mixture prior to blending. The mixed resin was coated on an aluminum plate or a Teflon disk followed by spinning at 3000 rpm for 10 s using a spin-coater (KW-8A, CHINAPONY Co. Ltd., China) to produce a smooth surface. The coated specimens were evaporated in an air chamber overnight to remove any small molecular residuals and then cured using a programmed temperature sequence (30 min at 25 °C, 45 min at 75 °C, and 135 min at 150 °C).[24−26] All the cured specimens were kept in

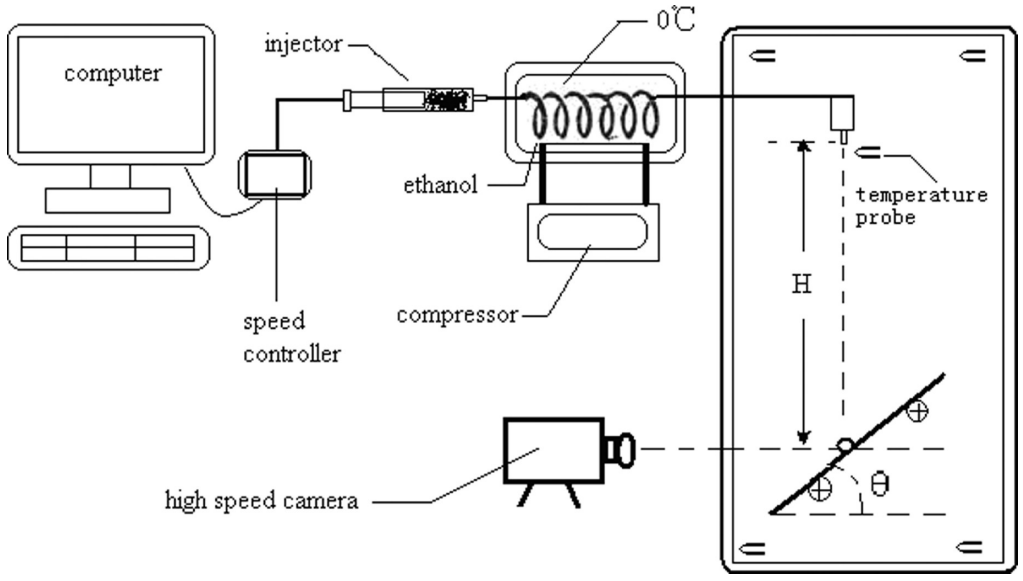

Figure 1. Schematic diagram of the set up for monitoring icing dynamics of a water droplet on a surface.

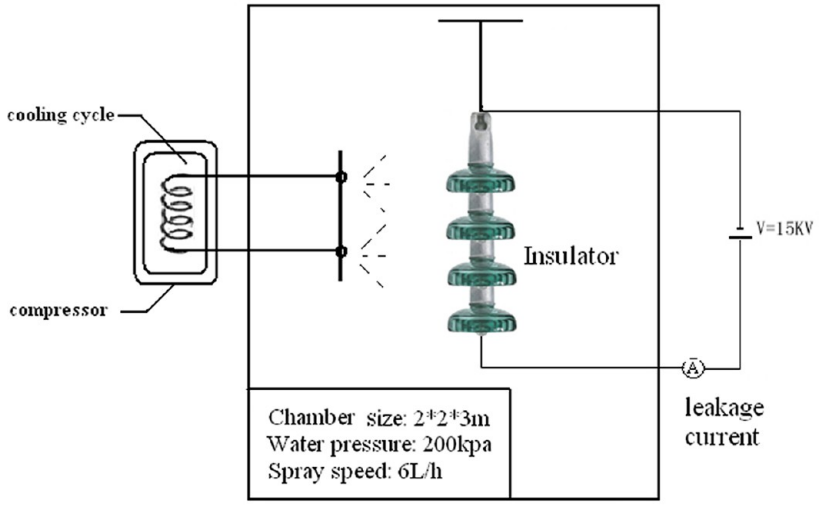

Figure 2. Schematic diagram of the ice accretion test on an insulator.

desiccators until they were used or tested for avoiding dust contamination.

General Tests. The surface topology of the specimen was observed by SEM (Hitachi, S-4800, Japan). The internal structure of the coating layer was checked by TEM (Hitachi, JEM-2100, Japan). The mechanical strength was tested using INSTRON 3366 universal testing machine (Instron Corp., USA) in a temperature chamber. Static contact angle (CA),[9,10] and ice adhesion strength test were described in our previous work and also in the Supporting Information.[11] Fourier transform infrared (FT-IR) spectra were collected on a FT-IR spectrometer (Vertex 70, BRUKER, Germany).

Surface Icing Dynamics. The icing dynamics of a water droplet on a surface was monitored in a temperature−humidity chamber (Figure 1). The temperature inside the chamber was controlled at 0, −5, −10 °C with a humidity at 80 ± 2%. These different condensing conditions with low temperatures and a high humidity were used to mimic different freezing rain weathers.[27−30] A droplet at 0 °C from double-distilled water was dropped onto the sample surface. The temperature of the water droplet and the surface was monitored by placing a high sensitive temperature probe under the syringe needle and another near the sample surface. The volume of the water droplet is chosen as 15 μL, to mimic raindrops in the nature. The behavior of a water droplet near and on the surface, including approaching and touching the surface, spreading, constricting and completely freezing on the surface was monitored by a high-speed camera (Phantom V-710, USA) operated at the speed of 4000 frames per second.

Icing on an Insulator. The ice accretion on an insulator was tested in a high voltage chamber (2 × 2x3 m) at −5 °C (Figure 2) in Shenzhen Graduate School, Tsinghua University. Supercooled water (at −5 °C) was sprayed to an insulator at a speed of 6L/h for 2h, whereas voltage was maintained at 15 KV, with the leakage current kept between 0.15 and 0.30 mA.

RESULTS AND DISCUSSION

Chemical Structures of Coating Materials. Polysiloxane is widely used for coatings and adhesives in a form of moisture curing resins. This type of curing system introduces a large amount of polar groups into the polymer for providing reactivity for curing. Unfortunately, these polar groups will also promote the surface interaction with water by hydrogen bonding and van der Waals forces, which will apparently increase the adhesion of ice with the surface. This interaction should be avoided for ice-phobic applications. Therefore, a curing system based on the platinum-catalyzed addition of vinyl with Si−H groups was

dx.doi.org/10.1021/am400704z | ACS Appl. Mater. Interfaces 2013, 5, 4053−4062

Scheme 2. Curing Mechanism Based on the Pt Catalytic Addition Reaction between Vinyl Group in PDMS-V and Si−H Group in PDMS-H

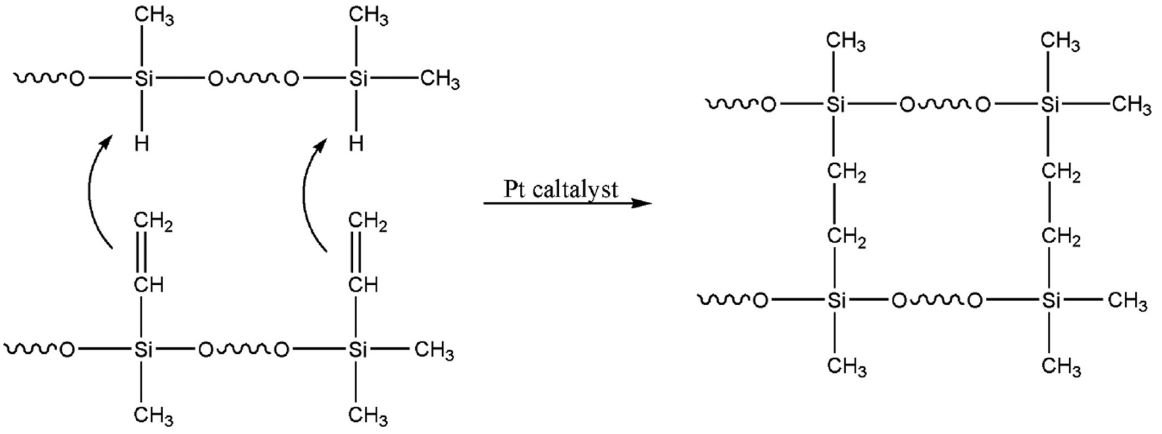

Scheme 3. Surface Modification of the Silica Particles by Reacting with D4

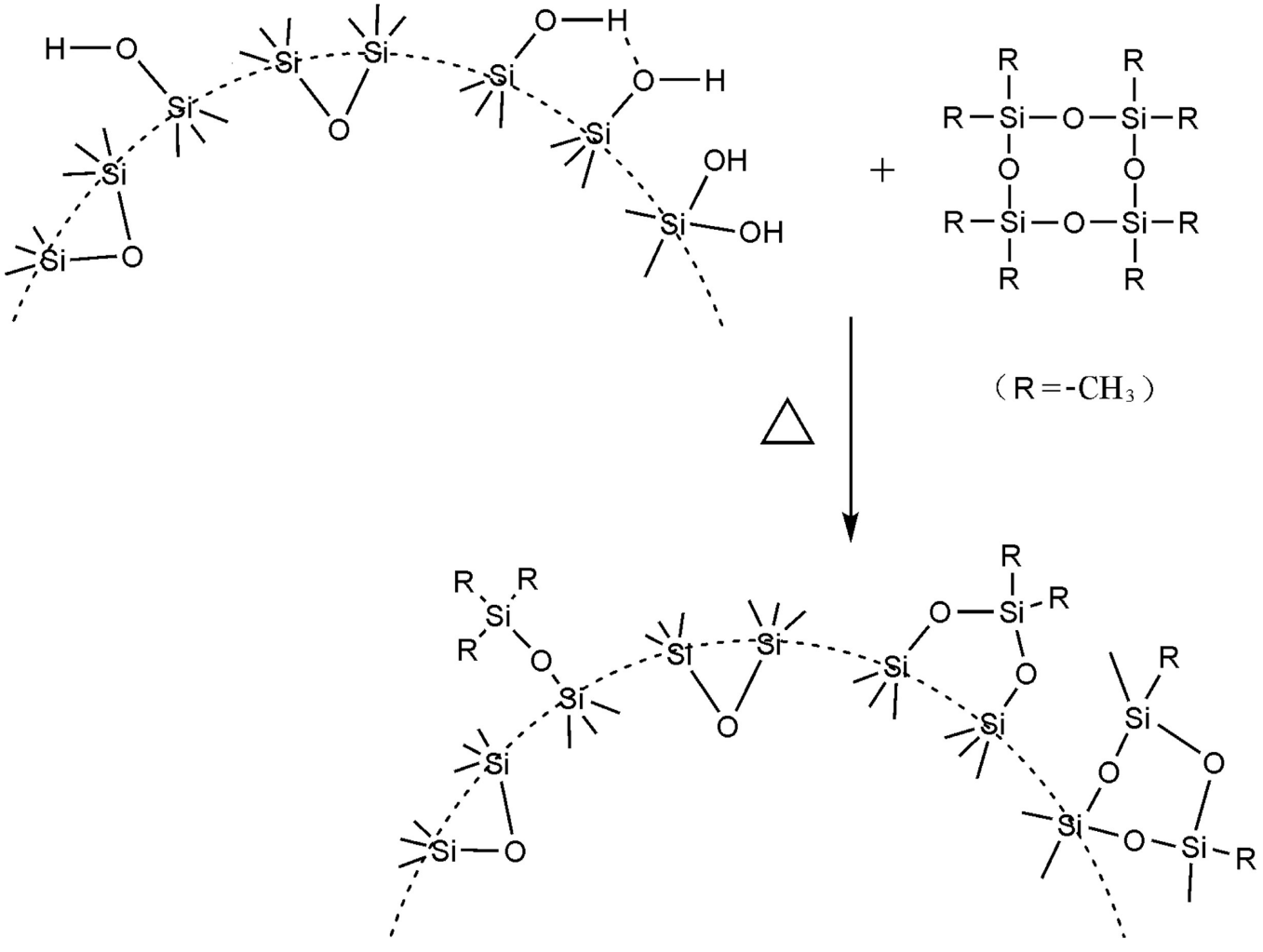

introduced into the resin. This work was started from the preparation of a vinyl containing PDMS (PDMS-V) and a Si−H containing PDMS (PDMS-H). In the presence of a platinum catalyst, the vinyl group in PDMS-V and the Si−H group in PDMS-H of the mixed resin will couple together to form an ethylene linkage to cross-link the polymer as indicated in Scheme 2. This curing system does not contain and generate any polar groups such as C═O and OH, so that a low surface energy of the final coating will be maintained to obtain a surface with a minimized ice adhesion strength. The absence of the polar groups in the formulated resins, Parts A and B was confirmed by FT-IR spectroscopy (see Figure S2 in the Supporting Information). These spectra did not show any characteristic absorption of polar groups.

To obtain an improved physical property of the coating layer and introduce nanoscale roughness to the coating surface, silica

nanoparticles (nano-SiO_2) were introduced into the resin. Following the same consideration as for the PDMS resin design, the polar OH group on the silica particle surface should be sealed off to reduce the interaction with water and ice. Therefore, the raw silica particles were treated with D4 at 180 °C (240 °C bath temperature) to eliminate the abundant OH groups on the surface as illustrated in Scheme 3. The reaction under this condition will only allow D4 to react with the OH group on silica gel surface to attach the fragments from D4 on the surface as illustrated in Scheme 3, but will not cause any polymerization of D4. Consequently, the surface-modified silica particles are easily isolated from the reaction mixture by filtration. This surface modification will also improve the compatibility of nano-SiO_2 with the polymer and promote the dispersion of the silica particles in the polymer matrix.

The success of the surface modification was confirmed by FT-IR spectroscopy.[31] The spectra of the pristine silica and the modified one were compared in Figure S1 in the Supporting Information. It showed that the characteristic absorption peak of OH group (3520 cm^{-1}) disappeared after being treated with D4, and new peaks at 2963, 2905, 1520, 1749, 1265, and 1318 cm^{-1} indicated that the silica gel surface was protected by the siloxane with the Si−OH group eliminated.

Surface and Bulk Morphology and Physical Strength of the PDMS Coating. Although a binary nano/microstructure is required for a superhydrophobic surface to create a highly water repelling property, this type of the surface structure is proved ineffective in preventing ice formation on the surface under a highly condensing condition with a lower temperature and a high humidity. It was found that moisture easily condensed and then formed icicles in the interspaces between the submicrometer grainlike or spherical protrudes of a superhydrophobic surface, these icicles further induced the icing process on the surface to root the surface ice into the rough surface structure. Extra force would be required to break down this icicle rooted ice layer on the surface. Therefore, eliminating the moisture condensation inside these submicrometer interspaces by either removing this structure or preventing the moisture condensation will be beneficial for reducing ice adhesion. A recently reported LIPS technique emerges a great potential to maintain the water-repelling property of a superhaydrophobic surface, and a high ice-repelling property by eliminating water condensation in the porous surface structure. The LIPS material is designed by infusing a water immiscible liquid into the porous structure of a superhydrophobic surface, so that topologically the surface is smooth. However, because of the immiscibility of the infused liquid with water, the surface will maintain a high water contact angle. The surface will also have a very small contact area between the solid substrate and water, since water mostly contact with the mobile water immiscible liquid. These characteristics make the LIPS to offer the surface a good water and ice repelling property, especially under a condensing weather condition. Therefore, in this work, we introduces a LIPS analogous coating based on silicon oil infused PDMS, where the large free volume of PDMS serves as voids to accommodate the silicon oil and to offer channel for it to migrate. The extremely low surface tension of the silicon oil and its occupation on the surface make the coating to have very low affinity with water and ice, so that this coating is expected to have a high ice-phobic property. On the other hand, to investigate the influence of the structure on the water and ice-repelling property of these materials, we will also first discuss the surface and bulk morphological structures of the PDMS coating without infused silicone oil.

The thickness of the PDMS coating was measured using AFM (image not shown), and an average thickness of 100 nm was observed for the spin-coated films. The topologic structure of the coating surface was investigated by SEM with the image shown in Figure 3b. It showed that the surface was smooth in micrometer

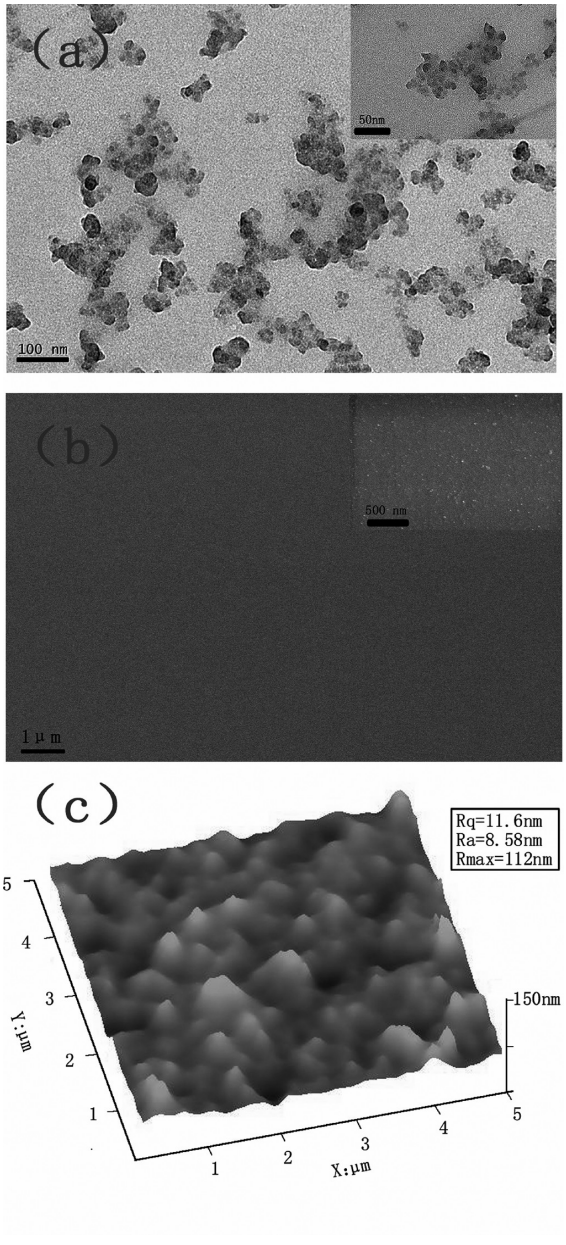

Figure 3. Morphology of the cross-linked PDMS coating reinforced with silica particles: (a) TEM image of a cross-section sample; (b) SEM images of the coating surface;(c) AFM image of the coating surface with R_q = 11.6 nm, R_a = 8.58 nm, and R_{max} = 112 nm.

scale, but a certain roughness in submicrometer scale. This was further investigated using AFM, and the image in Figure 3c showed that nanosized protrudes formed on the surface because of the existence of silica particles, which produced a root-mean-square roughness (R_q) of 11.6 nm, and standard deviation (R_a) of 8.58 nm. This result was verified by TEM study of a cross section sample. The image in Figure 3a shows that silica particles are distributed uniformly in the polymer matrix and no large-scale aggregates of the nano-SiO_2 was observed. These results indicate

that the surface modification of nano-SiO_2 has successfully improved its compatibility with PDMS, and created good dispersion of nano-SiO_2 in the polymer matrix. This effect was also proved by the physical strength test of the coating film using Instron with the result shown in Figure 4. It shows that the tensile

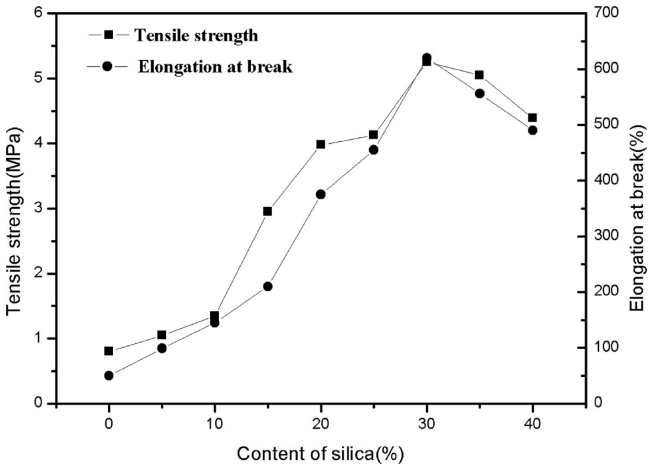

Figure 4. Influence of silica particle loading on the tensile strength and elongation of the silica-particle-reinforced PDMS coating film tested by Instron. Both tensile strength and elongation at break appear to reach maximum at 30% of silica content.

strength of the coating film is enhanced with the increase of the amount of nano-SiO_2 until 30% of silica content is reached, where a maximum value of 5.3 MPa is obtained, about 6 fold of the film without nano-SiO_2. This value is about 2 magnitudes greater than ice adhesion strength as will be discussed later, indicating that the coating is strong enough to resist the force for disrupting surface ice. Surprisingly, Figure 4 shows the elongation at break also significantly increase with the silica content and a maximum value of 620% was obtained at 30% of silica loading, which is about a 12-fold increase compared to the sample without silica particles. This property is extraordinary comparing to common engineering plastics, may be ascribed to the weak molecular interaction between polymer chains of pure PDMS, which will result in a low tensile strength and small elongation at break. The well-dispersed silica particles will act as physical cross-linking sites to enhance the interaction between the PDMS chains. In addition to the high flexibility of the PDMS chains, this interaction will promote not only tensile strength but also the elongation at break. This property in reverse proves that the silica particles are well-dispersed in the PDMS matrix.

Water Impact and Icing Dynamics on the Surfaces. It was found the icing process of water droplets on a cold surface has a significant influence on morphology of the formed ice, and thus had a great impact on the adhesion strength of the ice with the surface. Therefore, the icing dynamics of a water droplet at freezing point (0 °C) on the PDMS coating and aluminum surface were compared using a high speed camera.[32,33] To mimic the nature rainfall process in cold weather, this test was conducted in a temperature−humidity chamber at a temperature of 25, 0, −5, and −10 °C with a relative humidity of 80 ± 2% using 15 μL water droplets. The impact height of the water droplets was set at 5, 10, and 20 cm, respectively, to offer the droplet a different impact force. The behavior of a water droplet from approaching the surface to completely freezing was recorded by high speed photography. It showed that the water droplet would spread first on the surface driving by the impact force and then constrict due to the surface tension, and followed by several spreading/constricting cycles until an equilibrium contact angle reached. Several parameters including instant contact angle, the total spreading and constricting cycle numbers, the equilibrium contact angle, and the time for reaching the equilibrium were extracted from the photography. Figure 5

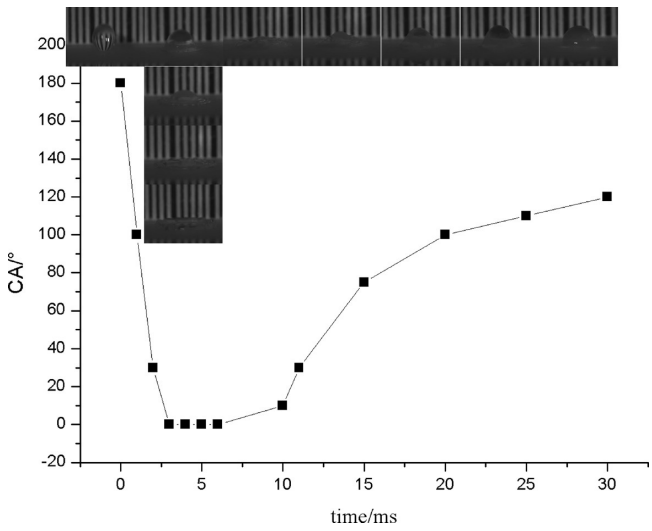

Figure 5. Instant contact angle variation of a 0 °C water droplet on the coating surface in the first cycle after impact in a 25 °C chamber.

recorded the variation of instant contact angle with tome on the PDMS surface of a water droplet in the first cycle as soon as it impacted the surface at a chamber temperature of 25 °C with 25 cm impact height. It showed that the droplet spread with the instant CA approaching 0° driven by the impact force and then it constricted to complete the first cycle in about 30 ms. The spreading of the droplet increased the covered area up to 10.9, 8.0, and 7.0 mm in diameter from 25, 10, and 5 cm impact height, respectively.

Figure 6 compared the total spreading/constricting cycle numbers before an equilibrium contact angle reached on PDMS coating and bare Al surface at temperatures of 25, 0, −5, and −10 °C. It shows the highest spreading/constricting cycling number of 55 on the coating surface at 5 cm impact height in a 25 °C chamber among the all tests. This number reduced with the increase of the impact height and decrease of the temperature, and was only 5 cycles at the impact height of 20 cm and the temperature of −10 °C on the same surface. When the surface was changed to bare Al, this number declined to 24 cycles at impact height of 5 cm and 25 °C, and further reduced to 2 cycles at impact height of 20 cm and 0 °C. When the temperature became lower than 0 °C, the behavior of a droplet became more complicated because of the quick freezing of the droplet. In this case, the water droplet was frozen on the surface in less than two cycles at −5 and −10 °C with impact heights of 10 and 20 cm. This result indicates that a droplet will undergo more spreading/constricting cycles on a lower energy surface with a lower impact force and at a higher temperature. It also shows that a water droplet can reach an equilibrium CA on the coated surface before freezing, even at −10 °C, whereas it can not on the bare Al surface at −5 and −10 °C.

On the other hand, Figure 7 displays the equilibrium time for a water droplet to reach the equilibrium contact angle after impact. It shows that a shorter equilibrium time is required on a lower

dx.doi.org/10.1021/am400704z | ACS Appl. Mater. Interfaces 2013, 5, 4053−4062

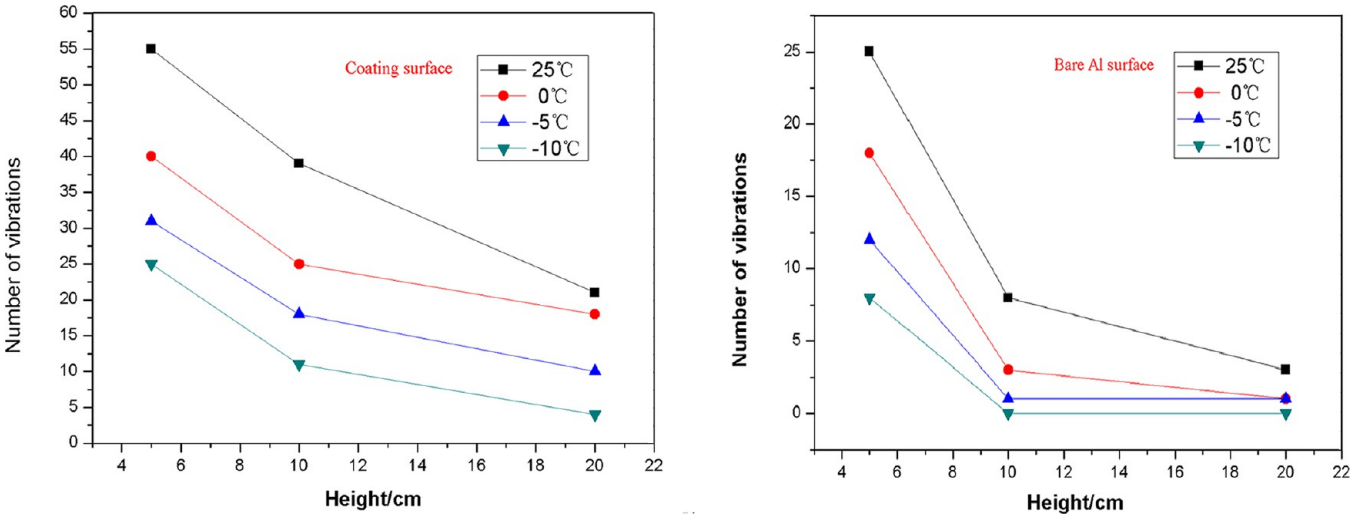

Figure 6. Total numbers of spreading/constricting cycles of a 25 °C water droplet on coated and bare Al surface at 25, 0, −5, and −10 °C before it reached an equilibrium CA.

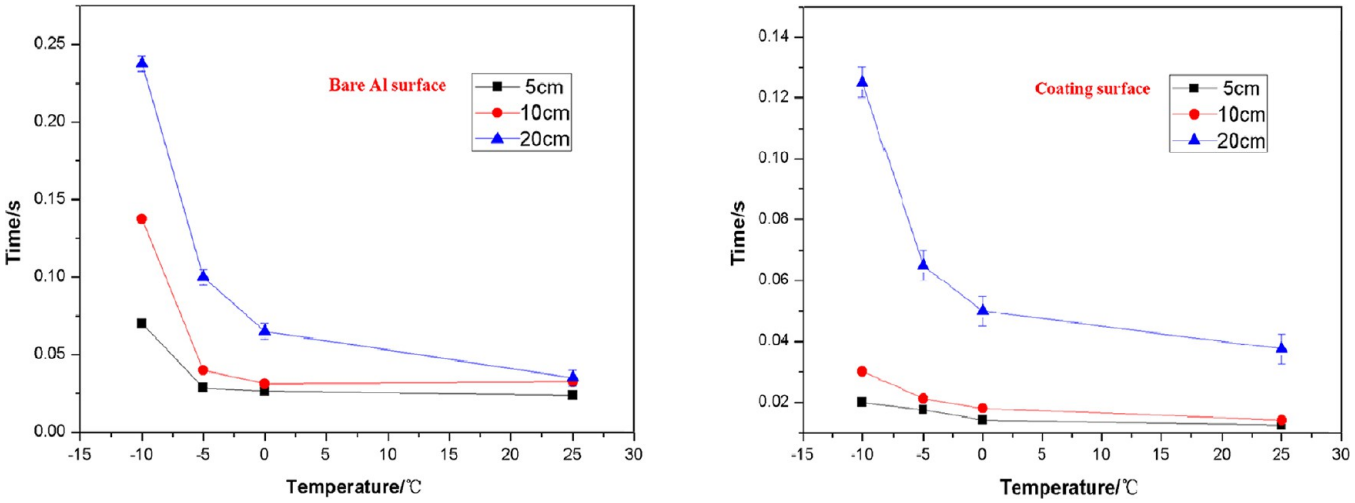

Figure 7. Equilibrium time for a 0 °C water droplet to reach the constant CA on the PDMS coating and bare Al surfaces in a chamber at 25, 0, −5, and −10 °C.

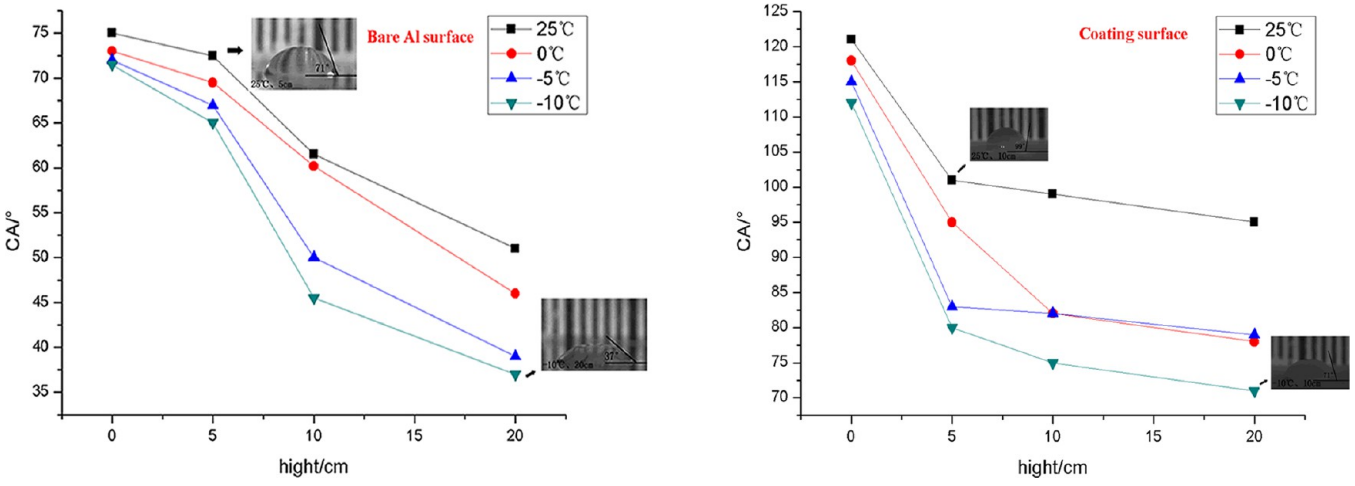

Figure 8. Constant contact angle of a water droplet on the PDMS coating and bare Al surfaces with different impact heights and temperatures.

energy surface with a lower impact height. For example, the equilibrium time is about 240 ms on a bare Al surface with 20 cm impact height at −10 °C. This value is reduced to about half (120 ms) on the PDMS coating surface at a same condition, and

dx.doi.org/10.1021/am400704z | ACS Appl. Mater. Interfaces 2013, 5, 4053−4062

further reduced to 20 ms with the impact height decreased to 5 cm. This result indicates that a water droplet on a lower energy surface will have sufficient time to reach an equilibrium contact angle before it is frozen, so that a small contact area of the formed ice can be obtained. This behavior apparently benefits for reducing the adhesion strength of the formed ice with the surface. This result, on the other hand, also explains the fact that a water droplet freezes much slower on PDMS coating surface than on bare Al surface. In conclusion, a low-energy surface has 2-fold effects for reducing the ice adhesion strength: (1) a much faster speed for a water droplet to reach the equilibrium CA with a small contact area, which leads to (2) a much slower cooling speed to offer the water droplet enough time to reach the equilibrium CA before freezing.

The equilibrium CA of a water droplet on the PDMS coating and bare Al surfaces at temperature of 25, 0, −5, and −10 °C is compared in Figure 8. On both PDMS coating and bare Al surfaces, the equilibrium CA decreases with raising impact height and reducing temperature. But the values on the coated surface are much higher than on the bare Al surface, in a range from 70 to 120° under all the testing conditions, whereas this value on the bare Al surface ranges only from 30 to 75°. In addition, with much shorter equilibrium time for a droplet to reach a constant contact angle than the time for a droplet to freeze as reported in our previous work,[34] this result means that a water droplet on the PDMS coating surface at −10 °C can still sufficiently constrict to a spherical shape and then start to freeze and finally become an ice ball with a small contact area with the surface. But on the surface of Al, the droplet at this temperature will spread out and freeze to form an ice layer. This effect will lead to the formation of a loose ice layer on the PDMS-coated surface, whereas a compact ice layer will form on the bare Al surface; this can be clearly evidenced by the ice accretion on an insulator under a highly condensing weather condition shown in Figure 9, where −5 °C

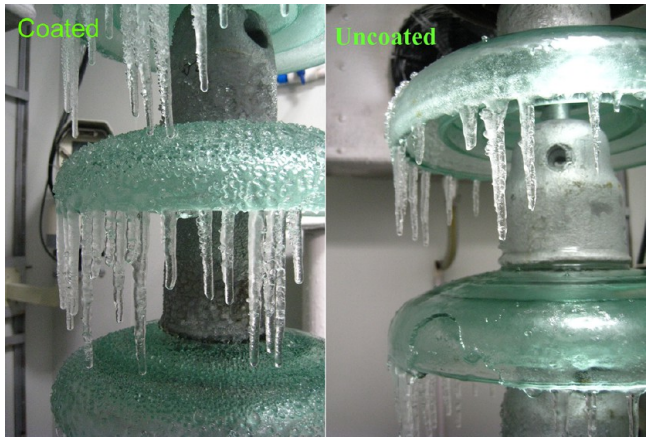

Figure 9. Ice formed on PDMS coated and uncoated surface of an insulator under a condensing weather condition at −5 °C and saturated humidity.

water was sprayed to an insulator at −5 °C and saturated humidity, and the ice formation was observed. It showed loose ice was formed on the coated surface and compact ice on the uncoated surface.

Ice Adhesion Strength. The ice adhesion was studied on bare Al, PDMS coating, and silicon-oil-infused PDMS coating. Figure 10 compares the ice adhesion tensile strength and shear strength of these surfaces. Compare to the bare Al, both tensile

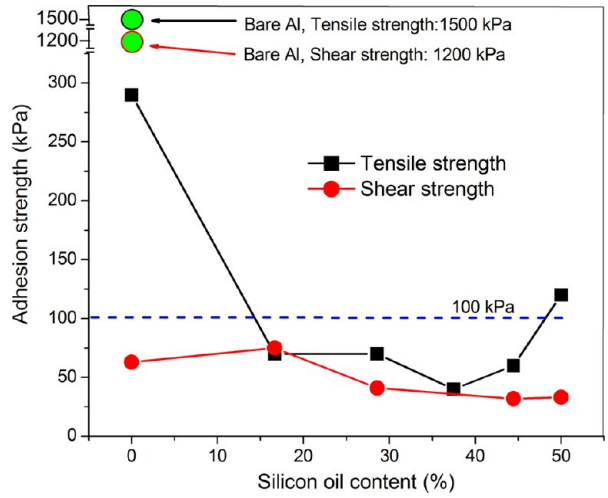

Figure 10. Tensile and shear strength of ice adhesion on the PDMS coating surfaces with different content of silicon oil.

and shear adhesion strength on PDMS coating surfaces fall drastically from 1500 to 290 kPa and from 1210 to 55 kPa. Furthermore, these values continue dropping to below 75 kPa (tensile) and 40 kPa (shear) on the silicon oil infused coating with silicon oil content higher than 20 wt %, dropped by a factor of 95%. This value is much lower than 100 kPa, a reference to judge if covered ice can be disrupted by a nature force such as wind, gravity, and so on or easily removed by consuming little energy. The much lower ice adhesion strength on the silicone oil infused coating surface is attributed to two factors: (1) the formation of a LIPS analogous coating surface; (2) reduced contact angle of the coating due to the low surface tension of PDMS and silicon oil, which will be proved by a static contact angle analysis in the following discussion. It was also observed that the ice-phobic property of the silicon oil infused coating was very durable, and the low ice adhesion strength could be maintained after a multiple deicing process. We believe this high durability is associated with the high mobility of the silicon oil in the coating, the extremely large free volume of the PDMS allow the silicon oil to migrate to surface for maintaining the LIPS analogous structure as soon as the silicon oil on the surface was lost in the deicing process. This behavior is schematically illustrated in Figure 11.

The effect of silicon oil to the contact angle is demonstrated in Figure 12. This test was conducted at both 25 °C and −10 °C with the coating containing different amount of silicon oil. At 25

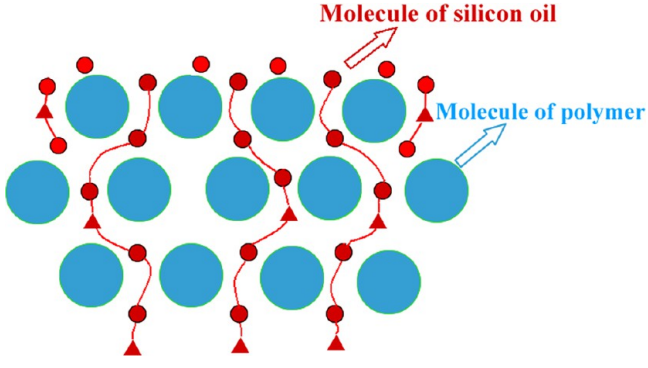

Figure 11. Regeneration of the LIPS analogous structure of the silicon oil infused PDMS coating by the migration of silicon oil to the surface.

dx.doi.org/10.1021/am400704z | ACS Appl. Mater. Interfaces 2013, 5, 4053−4062

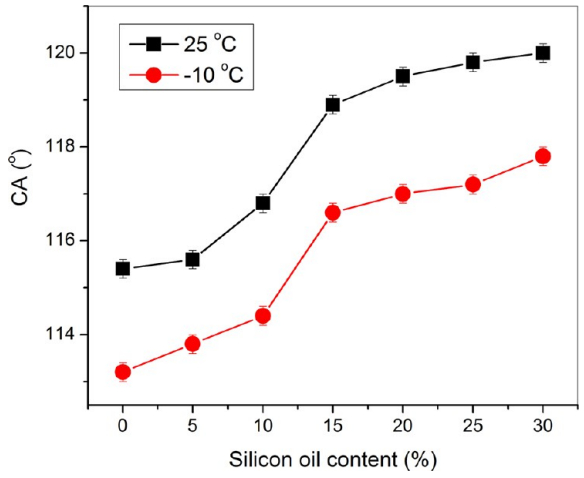

Figure 12. CA of the coating with different ratios of silicon oil at 25 °C and −10 °C.

°C and 43 ± 5% relative humidity, the contact angle of the coating slightly increases from 115.4 to 120.5° with the silicone oil content increased from 0 to 30 wt %. At −10 °C, Figure 12 exhibits the same tendency, but slightly lower CA values increases from 113.2 to 118.0°. It indicates that the water-repellent property can be improved by adding silicone oil. This result might be associated with better coverage of the silicon oil layer on the surface with the silicon oil content increased in the film. Silicon oil is a low molecular weight PDMS, possesses the same chemical structure and a similar surface tension as the high molecular weight PDMS matrix. The infused silicon oil will effectively screen off the defects on the surface, where polar structures such as those formed by broken silica particles may be exposed and thus ensure a perfect nonpolar surface with a low surface tension. This result also means that the effect of the silicon oil on the contact angle has a good correlation with its effect on the ice-phobic property, proposing a LIPS analogous surface from the silicon oil infused PDMS coating.

CONCLUSION

(1) A PDMS resin with a curing system based on the Pt catalyzed addition of vinyl with Si−H groups has been introduced. This system does not introduce any polar group into coating and thus ensures a low interaction with water and ice, leading to a low surface energy and a highly hydrophobic property with a contact angle of 115°.

(2) PDMS coatings have been prepared from this resin with the addition of surface modified silica particles to produce a nanoscale surface roughness. This surface has very low ice adhesion with a tensile strength of 0.29 MPa and a shear strength of 0.06 MPa.

(3) Silicon-oil-infused PDMS coatings have been introduced to further reduce the ice adhesion strength. When 20−40 wt % silicon oil was added, the ice adhesion tensile strength is lower than 0.075 MPa, only about 5% on bare Al surface. This effect was associated with the formation of a surface with an analogous structure as liquid infused porous surface (LIPS).

(4) Because of a high speed of spreading/constricting vibration and a low freezing rate, a water droplet can easily reach an equilibrium contact angle with a high value on the PDMS coating surface. This makes the frozen water droplet had a small contact area, and thus leads to a loose ice layer formed on the surface.with a low adhesion strength, this type of ice will be easily removed from the surface, even by nature force such as vibration, wind, and gravity. As comparison, the ice formed on a bare aluminum surface under the same condition is much more compact and strong.

ASSOCIATED CONTENT

Supporting Information

FTIR spectra of the pristine and modified silica particles, PDMS resin, and experimental details for ice adhesion tensile and shear strength tests. This material is available free of charge via the Internet at http://pubs.acs.org.

AUTHOR INFORMATION

Corresponding Author

*Tel.: +86 25 83593289. Fax: +86 25 83593048. E-mail: njuwqj@nju.edu.cn.

Notes

The authors declare no competing financial interest.

ACKNOWLEDGMENTS

This work is supported by Nanjing University Testing fund and Yunnan Electric Power Test & Research Institute fund. The authors are grateful to Dr. Zhou for technical assistance with TEM measurements and to Dr. Wang for valuable comments.

REFERENCES

(1) Guo, P.; Zheng, Y.; Wen, M.; Song, C.; Lin, Y.; Jiang, L. *Adv. Mater.* **2012**, *24*, 2642−2648.
(2) Stone, H. A. *ACS Nano* **2012**, *6*, 6536−6540.
(3) Blackburn, R. R.; Kinzig, B. J.; Schmidt, C. G. *Strategic Highway Research Program*; National Research Council: Washington, D.C., 1993; Vol. 4, p 9.
(4) Ferrick, M. G.; Mulherin, N. D.; Haehnel, R. B.; Coutermarsh, B. A.; Durell, G. D.; Tantillo, T. J.; Curtis, L. A.; Clair, T. L. S.; Weiser, E. S.; Cano, R. J.; Smith, T. M.; Martinez, E. C. *Cold. Reg. Sci. Technol.* **2008**, *52*, 224−243.
(5) Cao, L.; Jones, A. K.; Sikka, V. K.; Wu, J.; Gao, D. *Langmuir* **2009**, *25*, 12444−12448.
(6) Jung, S.; Tiwari, M. K.; Doan, N. V.; Poulikakos, D. *Nat. Commun.* **2012**, *3*, 615.
(7) Chen, J.; Liu, J.; He, M.; Li, K.; Cui, D.; Zhang, Q.; Zeng, X.; Zhang, Y.; Wang, J.; Song, Y. *Appl. Phys. Lett.* **2012**, *101*, 111603.
(8) Li, K.; Xu, S.; Shi, W.; He, M.; Li, H.; Li, S.; Zhou, X.; Wang, J.; Song, Y. *Langmuir* **2012**, *28*, 10749−10754.
(9) Yin, L.; Wang, Q.; Xue, J.; Ding, J.; Chen, Q. *Chem. Lett.* **2010**, *39*, 816−817.
(10) Yin, L.; Zhu, L.; Wang, Q.; Ding, J.; Chen, Q. *ACS Appl. Mater. Interfaces* **2011**, *3*, 1254−60.
(11) Yang, S.; Xia, Q.; Zhu, L.; Xue, J.; Wang, Q.; Chen, Q.m. *Appl. Surf. Sci.* **2011**, *257*, 4956−4962.
(12) Jung, S.; Dorrestijn, M.; Raps, D.; Das, A.; Megaridis, C. M.; Poulikakos, D. *Langmuir* **2011**, *27*, 3059−3066.
(13) Nosonovsky, M.; Hejazi, V. *ACS Nano* **2012**, *6*, 8488−8491.
(14) Kim, P.; Wong, T. S.; Alvarenga, J.; Kreder, M. J.; Adorno-Martinez, W. E.; Aizenberg, J. *ACS Nano* **2012**, *6*, 6569−6577.
(15) Wong, T. S.; Kang, S. H.; Tang, S. K.; Smythe, E. J.; Hatton, B. D.; Grinthal, A.; Aizenberg, J. *Nature* **2011**, *477*, 443−447.
(16) Bahadur, V.; Mishchenko, L.; Hatton, B.; Taylor, J. A.; Aizenberg, J.; Krupenkin, T. *Langmuir* **2011**, *27*, 14143−14150.
(17) Ramezanzadeh, B.; Mohseni, M.; Mohammad Rabea, A.; Yari, H. *Int. J. Adhes. Adhes.* **2011**, *31*, 775−783.
(18) Xiu, Y.; Zhu, L.; Hess, D. W.; Wong, C. P. *Nano Lett.* **2007**, *7*, 3388−3393.

(19) Arkles, B.; Crosby, J. *Polysiloxane Thermoplastic Interpenetrating Polymer Networks*; American Chemical Society: Washington, D.C., 1990; Vol. *224*, pp 181−199.
(20) Dumont, M. F.; Moisan, S.; Aymonier, C.; Marty, J. D.; Mingotaud, C. *Macromolecules* **2009**, *42*, 4937−4940.
(21) Kaneko, M. L. Q. A.; Romero, R. B.; Gonçalves, M. D. C.; Yoshida, I. V. P. *Eur. Polym. J.* **2010**, *46*, 881−890.
(22) Kenawy, E. R.; Hay, F. I. A; Shanshoury, A. E. R.; Newehy, M. H. *J. Polym. Sci., Part A: Polym. Chem.* **2002**, *40*, 2384−2393.
(23) Lewis, B. L. N.; Stein, J.; Gao, Y.; Colborn, R.; Gudrun, H. *Platinum Met. Rev.* **1997**, *41*, 66−75.
(24) Chen, J.; Wu, W.; You, Y.; Fan, W.; Chen, Y. *J. Appl. Polym. Sci.* **2010**, *117*, 2964−2971.
(25) Pavlyuchenko, V. N.; Sorochinskaya, O. V.; Ivanchev, S. S.; Khaikin, S. Y.; Trounov, V. A.; Lebedev, V. T.; Sosnov, E. A.; Gofman, I. V. *Polym. Adv. Technol.* **2009**, *20*, 367−377.
(26) Quaranta, A.; Carturan, S.; Marchi, T.; Cinausero, M.; Scian, C.; Kravchuk, V. L.; Degerlier, M.; Gramegna, F.; Poggi, M.; Maggioni, G. *Opt. Mater.* **2010**, *32*, 1317−1320.
(27) Kako, T.; Nakajima, A.; Irie, H.; Kato, Z.; Uematsu, K.; Watanabe, T.; Hashimoto, K. *J. Mater. Sci.* **2004**, *39*, 547−555.
(28) Varanasi, K. K.; Deng, T.; Smith, J. D.; Hsu, M.; Bhate, N. *Appl. Phys. Lett.* **2010**, *97*, 234102.
(29) Karmouch, R.; Ross, G. G. *J. Phys. Chem. C* **2010**, *114*, 4063−4066.
(30) Zheng, L.; Li, Z.; Bourdo, S.; Khedir, K. R.; Asar, M. P.; Ryerson, C. C.; Biris, A. S. *Langmuir* **2011**, *27*, 9936−9943.
(31) Fang, X.; Huang, X.; Lu, Z.; Chen, L.; Chen, S. *Polym. Compos.* **2010**, *31*, 1628−1636.
(32) Mishchenko, L.; Hatton, B.; Bahadur, V.; Taylor, A.; Krupenkin, T.; Aizenberg, J. *ACS Nano* **2010**, *4*, 7699−7707.
(33) Alizadeh, A.; Bahadur, V.; Zhong, S.; Shang, W.; Li, R.; Ruud, J.; Yamada, M.; Ge, L.; Dhinojwala, A.; Sohal, M. *Appl. Phys. Lett.* **2012**, *100*, 111601.
(34) Yin, L.; Xia, Q.; Xue, J.; Yang, S.; Wang, Q.; Chen, Q. *Appl. Surf. Sci.* **2010**, *256*, 6764−6769.